

Wang-Landau Monte Carlo simulation of isotropic-nematic transition in liquid crystals

D. Jayasri,¹ V. S. S. Sastry,¹ and K. P. N. Murthy²

¹*School of Physics, University of Hyderabad, Hyderabad 500 046 Andhra Pradesh, India*

²*Materials Science Division, Indira Gandhi Centre for Atomic Research, Kalpakkam 603 102, Tamilnadu, India*

(Received 31 March 2005; published 8 September 2005)

Wang and Landau proposed recently, a simple and flexible non-Boltzmann Monte Carlo method for estimating the density of states, from which the macroscopic properties of a closed system can be calculated. They demonstrated their algorithm by considering systems with discrete energy spectrum. We find that the Wang-Landau algorithm does not perform well when the system has continuous energy spectrum. We propose in this paper modifications to the algorithm and demonstrate their performance on a lattice model of liquid crystalline system (with Lebwohl-Lasher interaction having continuously varying energy), exhibiting transition from high temperature isotropic to low temperature nematic phase.

DOI: [10.1103/PhysRevE.72.036702](https://doi.org/10.1103/PhysRevE.72.036702)

PACS number(s): 64.70.Md, 05.10.Ln

I. INTRODUCTION

Monte Carlo methods have emerged as a powerful and reliable tool for simulating several complex phenomena in statistical physics, see, e.g., Refs. [1,2]. The Metropolis algorithm [3] discovered in the middle of the last century can be considered as the starting point. This algorithm generates a Markov chain, the asymptotic part of which contains microstates belonging to a canonical ensemble at a temperature chosen for the simulation. Expectation value of a macroscopic property can be estimated by taking a simple arithmetic average over a Monte Carlo sample. The associated statistical error is inversely proportional to the square root of the sample size. Thus, in principle, we can estimate a physical property to the desired accuracy by simply increasing the sample size. However, if successive microstates in the sampled Markov chain are correlated, the statistical error increases by a factor $\sqrt{1+2\tau^*}$, see, e.g., Ref. [4], where τ^* is the integrated correlation time. Such a situation occurs when we simulate a system close to criticality.

The Metropolis algorithm and its several variants like Glauber [5], heat-bath [6], and Kawasaki exchange [7] algorithms come under the class of Boltzmann sampling techniques. The limitations of Boltzmann sampling have long since been recognized. For example, it cannot address satisfactorily problems of critical slowing down, i.e., divergence of τ^* with increase of system size, near continuous phase transition. Cluster algorithms [8] overcome this problem. Boltzmann sampling is also not suitable for problems of super critical slowing down near first order phase transitions. The microstates representing the interface between ordered and disordered phases have intrinsically low probability of occurrence in a closed system and hence are scarcely sampled; switching from one phase to the other takes a very long time due to the presence of high energy barriers when the system size is large; as a result the relative free energies of ordered and disordered phases cannot be easily and accurately determined. Finally it is quite difficult to estimate the absolute values of entropy or free energies in Boltzmann sampling techniques.

A. Non-Boltzmann sampling

That non-Boltzmann sampling can provide a legitimate and often superior alternative to Boltzmann sampling was recognized even during the early days of Monte Carlo practice, see, e.g., Ref. [9]. However, the practical convenience and significance of non-Boltzmann sampling was appreciated only in the middle of the 1970s when Torrie and Valleau [10] proposed the so-called umbrella sampling; this is a forerunner to all the subsequent non-Boltzmann sampling techniques including the multicanonical Monte Carlo [11] and its several and recent variants. Entropic sampling [12], equivalent to multicanonical sampling [11], provides a transparent and intuitively appealing insight into non-Boltzmann Monte Carlo techniques. It is based on the following premise.

The probability that a closed system can be found in a microstate \mathcal{C} is given by

$$P(\mathcal{C}) = [Z(\beta)]^{-1} \exp[-\beta E(\mathcal{C})]. \quad (1)$$

In the above $E(\mathcal{C})$ is the energy of the microstate \mathcal{C} and $\beta = (k_B T)^{-1}$, where k_B is the Boltzmann constant and T is the temperature. $Z(\beta)$ is the canonical partition function given by

$$Z(\beta) = \sum_{\mathcal{C}} \exp[-\beta E(\mathcal{C})] = \int D(E) \exp(-\beta E) dE,$$

where $D(E)$ is the density of states. The probability density for a closed system to have an energy E is thus given by

$$P_B(E) \propto D(E) \exp(-\beta E), \quad (2)$$

where the suffix B indicates that it is the Boltzmann-Gibbs distribution (appropriate for modeling a closed system). Let us suppose we want to sample microstates in such a way that the resultant probability density of energy is given by

$$P_g(E) \propto D(E) [g(E)]^{-1}, \quad (3)$$

where $g(E)$ is chosen as per the desired non-Boltzmann distribution. Once $P_g(E)$ is known, an ensemble consistent with Eq. (3) can be constructed as follows.

Let C_i be the current microstate and C_t the trial microstate obtained from C_i by making a local change, e.g., flip a randomly chosen spin in Ising model simulation. Let $E_i=E(C_i)$ and $E_t=E(C_t)$ denote the energy of the current and of the trial microstate, respectively. The next entry C_{i+1} in the Markov chain is taken as

$$C_{i+1} = \begin{cases} C_t & \text{with probability } p, \\ C_i & \text{with probability } (1-p), \end{cases} \quad (4)$$

where the acceptance probability p is given by

$$p = \min \left[1, \frac{P_g(E_t)}{P_g(E_i)} \right] \equiv \min \left[1, \frac{g(E_t)}{g(E_i)} \right]. \quad (5)$$

We call this non-Boltzmann sampling with respect to a given $g(E)$. It is easily verified that the above acceptance rule obeys detailed balance. Hence the Markov chain constructed would converge asymptotically to the desired g ensemble.

When $[g(E)]^{-1} = \exp(-\beta E)$ we recover conventional Boltzmann sampling, implemented in the Metropolis algorithm. For any other choice of $g(E)$ we get the corresponding non-Boltzmann sampling. Now, canonical ensemble average of a macroscopic property $O(C)$ can be obtained by unweighting and reweighting of $O(C)$ for each C sampled from the g ensemble. For unweighting we divide by $[g(E(C))]^{-1}$ and for reweighting we multiply by $\exp[-\beta E(C)]$. The weight factor associated with a microstate C belonging to the g ensemble is thus,

$$W(C, \beta) = g(E(C)) \exp[-\beta E(C)]. \quad (6)$$

We then have

$$\langle O \rangle = \frac{\sum_C O(C) W(C, \beta)}{\sum_C W(C, \beta)}. \quad (7)$$

The left-hand side of the above is the equilibrium value of O in a closed system at β , while on the right-hand side the summation in the numerator and in the denominator runs over microstates belonging to the non-Boltzmann g ensemble. It is also clear that from a single simulation of a g ensemble, we can calculate the canonical average of O at various temperatures.

B. Entropic sampling

Entropic sampling obtains when $g(E)=D(E)$. This choice of $g(E)$ renders $P_g(E)$ the same for all E , see Eq. (3). The system does a simple random walk on a one-dimensional energy space. Hence all energy regions are visited with equal probability. As a result, in the case of first order phase transition for example, the microstates on the paths (in the configurational space) that connect ordered and disordered phases would get equally sampled. A crucial issue that remains to be clarified pertains to the observation that we do not know $D(E)$ *a priori*.

In entropic sampling we employ a strategy to push $g(E)$ closer and closer to $D(E)$, iteratively. We divide the range of

energy into a large number of bins of equal widths. We denote the discrete-energy version of $g(E)$ by the symbol $\{g_i: i=1, M_E\}$, where M_E is the number of energy bins. We start with $\{g_i^{(0)}=1 \forall i=1, M_E\}$; the superscript is iteration run index and the subscript is energy bin index. The aim is to update $\{g_i\}$ from one iteration to the next, $\{g_i^{(0)}\} \rightarrow \{g_i^{(1)}\} \rightarrow \dots \{g_i^{(k)}\} \rightarrow \dots$, so that asymptotically we get $\{g_i\}$ as close to $\{D_i\}$ as desired, where $\{D_i\}$ is the discrete energy representation of $D(E)$. The iteration is carried out as follows. In the k th iteration, for example, we generate a large number of microstates employing acceptance probability based on $\{g_i^{(k)}\}$, see Eq. (5), and accumulate a histogram $\{h_i: i=1, M_E\}$ of energy of visited microstates. We update $\{g_i^{(k)}: i=1, M_E\}$ to $\{g_i^{(k+1)}: i=1, M_E\}$, as given below,

$$g_i^{(k+1)} = \begin{cases} g_i^{(k)} & \text{if } h_i = 0, \\ g_i^{(k)} \times h_i & \text{if } h_i \neq 0, \end{cases} \quad (8)$$

for all $i=1, 2, \dots, M_E$. The updated $\{g_i^{(k+1)}\}$ is employed in the next, i.e., $(k+1)$ th run, during which a fresh histogram of energy is generated. After each run, the histogram is examined for its uniformity. Flatter the histogram, closer is $\{g_i\}$ to $\{D_i\}$. Thus, the calculated histogram serves two purposes in entropic sampling, one for updating $\{g_i\}$ and the other for monitoring the convergence of $\{g_i\}$ to $\{D_i\}$. However, often, it is neither practical nor necessary to get a strictly flat histogram; an approximately flat histogram would be adequate, thanks to the unweighting followed by reweighting with the Boltzmann rule while calculating the averages, see Eqs. (6) and (7). Hence the calculated macroscopic properties would come out right, even if $\{g_i\}$ does not converge strictly to $\{D_i\}$.

C. Wang-Landau algorithm

A simple and flexible variant to entropic sampling was proposed recently by Wang and Landau [13]. The distinguishing feature of this algorithm is the dynamic evolution of the acceptance probability, p ; we update $\{g_i\}$ after every Monte Carlo step. Let us say the system visits a microstate in a Monte Carlo step and let the energy of the visited microstate fall in the m th energy bin; then g_m is updated to $f \times g_m$, where f is the Wang-Landau factor, see below. The updated $\{g_i\}$ becomes operative immediately for determining the acceptance or rejection criteria from the very next trial move. We set $f=f_0$ for the zeroth run; f_0 can be any number greater than unity; the choice of $f_0=e$ has been originally recommended by Wang and Landau. We generate a large number of microstates employing the dynamically evolving p . At the end of a run we calculate the histogram of energy of microstates visited by the system during the run. Because of the continuous updating of p , the energy span of the density of states increases significantly and the energy histogram serves to monitor the convergence of $\{g_i\}$ to $\{D_i\}$. A run should be long enough to facilitate the system to span the energy over the desired range and to render the histogram of energy approximately flat. At the end of, say, the ν th run, the Wang-Landau factor for the next run is set as $f=f_{\nu+1}=\sqrt{f_\nu}$. After several runs, this factor would be very close to unity;

this implies that there would occur no significant change in $\{g_i\}$ during later runs. For example, with the square-root rule and $f_0=e$, we have $f_{25}=\exp(2^{-25})\approx 1+10^{-7}$. It is clear that f decreases monotonically with increase of the run index and reaches unity asymptotically. Wang and Landau have recommended the square-root rule [13]; any other rule consistent with the above properties of monotonicity and asymptotic convergence to unity should do equally well.

From the converged g , the desired macroscopic properties of the system can be calculated; to this end we invoke the connection between the density of states and microcanonical entropy, $\alpha(E)=k_B \log D(E)$. Thus the Monte Carlo estimate of microcanonical entropy is $k_B \log g(E)$. For implementing such a scheme we need to normalize $g(E)$. The normalization constant should be obtained from known properties of the system. For example, in the Ising model, the ground state is doubly degenerate, $D(E_{\min})=2$. The total number of microstates equals 2^V where V is the number of Ising spins in the Monte Carlo model, $\int_{E_{\min}}^{E_{\max}} D(E)dE=2^V$. Either of these known information can be employed for normalizing g . The normalized $g(E)$ provides a good approximation to $D(E)$.

Alternately, we can take the output $\{g_i\}$ from the above and carry out a single long non-Boltzmann sampling run which generates microstates belonging to the g ensemble. Note that during the production run we do not update $g(E)$. By unweighting and reweighting of the microstates generated in the production run, we calculate the desired properties of the system as a function of β . This is the strategy we shall follow for the simulation of the liquid crystal system, described in the rest of the paper. In this strategy, we can employ arbitrary normalization of g ; more importantly, it is adequate if

(a) the system visits the energy region of interest and not necessarily the entire range and

(b) the histogram of energy in the region of interest is approximately flat.

The usefulness of the Wang-Landau algorithm has been unambiguously demonstrated for systems with discrete energy spectrum. Indeed originally the Wang-Landau method was applied to the Ising model for which the possible energies are a discrete set of integers. However, when we try to apply this technique to systems with continuous energy, e.g., Lennard-Jones fluid/glass [17–19], Heisenberg spins [20], and protein simulation [21], there are serious difficulties. Liquid crystalline materials with continuous energy spectrum provide such an example. In this paper we report simulation of a liquid crystalline system focusing attention on nematic-isotropic transition. The paper is organized as follows. In Sec. II, we describe a lattice model and Hamiltonian of a liquid crystal system. We simulated the system with the conventional Wang-Landau algorithm, which implicitly involves discrete set of energies. Since the liquid crystal molecules are continuously orientable, the possible energies are real numbers. This complicates the estimation of density of states in the Wang-Landau algorithm. We find that the dynamics becomes extremely slow even for moderately large systems. The system gets stuck in certain regions of the configurational space. This problem appears to be generic to the algorithm when applied to continuous energy systems [17–20].

Hence we modify the Wang-Landau algorithm and the details of the simulation are given in Sec. III. The results on temperature variation of various macroscopic properties of the system are discussed in Sec. IV. In Sec. V we briefly summarize the work and highlight its salient features.

II. LATTICE MODEL OF BULK LIQUID CRYSTALS

We consider an $L \times L \times L$ cubic lattice with each lattice site holding a three-dimensional unit vector $|u\rangle$, called a spin. The elements of the vector are the direction cosines of a spin in a laboratory frame of reference. A spin represents notionally, a single uniaxial liquid crystal molecule or more realistically a cluster containing typically 100 of them. The spins are actually headless in the sense the system has head-tail flip symmetry. Two nearest neighbor spins interact with each other as per a potential proposed by Lebwohl and Lasher (LL) [14] which has such a head-tail flip symmetry. The interaction energy is given by

$$\epsilon_{i,j} = -\frac{1}{2}[3 \cos^2(\theta_{i,j}) - 1], \quad (9)$$

where i and j are nearest neighbor lattice sites. $\theta_{i,j}$ is the angle between the two spins, $\cos(\theta_{i,j})=\langle u_i | u_j \rangle$. The interaction energy of a single nearest neighbor pair of spins ranges from a minimum of -1 , when $\theta_{i,j}=0$, or equivalently $\langle u_i | u_j \rangle=1$, to a maximum of $+1/2$, when $\theta_{i,j}=\pi/2$ or equivalently $\langle u_i | u_j \rangle=0$. Total energy of the system in microstate C is given by

$$E(C) = \sum_{(i,j)} \epsilon_{i,j}, \quad (10)$$

where the sum runs over all distinct nearest neighbor pairs of lattice sites in the system taking into account the periodic boundary conditions in all three directions. The total energy of the system thus varies continuously from a minimum of $-3L^3$ to a maximum of $+3L^3/2$. When the system is completely ordered with all the spins aligned, the energy is minimum and equals $-3L^3$; the energy is zero for an isotropic (completely disordered) phase. We calculate several macroscopic properties of the liquid crystalline system and report here results which include orientational order parameter $\langle S \rangle$, average energy $\langle E \rangle$, specific heat (at constant volume) C_V , and the Binder's reduced fourth cumulant of energy V_4 .

First we employed conventional Wang-Landau algorithm and carried out Monte Carlo simulation of the lattice model of the liquid crystalline system. We found that the dynamics were extremely slow when the system size L is 6 and above. The calculated density of states $g(E)$ becomes steeper with increase of Monte Carlo iterations. As a result the system gets stuck in certain narrow regions. There is practically no evolution of the calculated density of states $g(E)$. Increasing the number of Monte Carlo steps in a Wang-Landau iteration does not seem to remedy the situation. Instead, sharp peaks emerge and grow at either ends of $g(E)$. These problems appear to be generic to the Wang-Landau algorithm when applied to continuous energy systems. To overcome them, we experimented with several modifications [16] of the algorithm and finally arrived at a strategy described in the next section.

We remark that need for improving and generalizing the Wang-Landau algorithm to different kinds of problems has been recognized. For example, a generalization of Wang-Landau algorithm to off-lattice simulation can be found in Ref. [17]. Extension of Wang-Landau algorithm to zero-field susceptibility calculations in Heisenberg spin model can be found in Ref. [20]; calculation of density of states of proteins from the so-called instantaneous configurational temperature has been employed in the application of Wang-Landau algorithm to protein simulation [21]; *etc.*

III. MODIFIED WANG-LANDAU MONTE CARLO SIMULATION OF BULK LIQUID CRYSTAL SYSTEM

Free wheeling spins are placed on the vertices of a three-dimensional cubic lattice with their orientations sampled randomly and independently. Orientation of a spin is specified by the polar angle θ and an azimuthal angle ϕ with respect to a laboratory fixed three-dimensional coordinate system. We sample $\mu = \cos(\theta)$ from a uniform distribution between 0 and 1, and the azimuthal angle ϕ from a uniform distribution between 0 and 2π . We divide the energy range $(-3L^3, +1.5L^3)$ into $M=9L^3$ number bins of equal widths $\Delta E=0.5$. We start with an array $\{g_i=e^2 \forall i=1, 9L^3\}$. Let C_0 denote the initial microstate constructed by placing spins with random and independent orientations at the lattice sites. Let $E(C_0)$ fall in the μ th energy bin. We select randomly a lattice site and make a random change in the orientation of the spin residing at that site. We employ Barker's method [22] to generate a new trial orientation from the current microstate. Barker's method essentially consists of selecting randomly and with equal probability one of the three Cartesian axes and rotating the liquid crystal molecule by an angle $\Delta\theta$ radians about this axis. $\Delta\theta$ is uniformly distributed between -0.5 and $+0.5$ radians. Let C_t denote the trial microstate and let its energy belong to the ν th bin. If $g_\nu \leq g_\mu$, we accept the trial state and set $C'_1=C_t$; if $g_\nu > g_\mu$, we calculate the ratio $p = g_\mu/g_\nu$. We select a random number r (uniformly distributed between 0 to 1); if $r \leq p$ we accept the trial microstate, $C'_1=C_t$. Otherwise we reject C_t and set $C'_1=C_0$. This constitutes a single move. We continue in the same fashion and get $C_0 \rightarrow C'_1 \rightarrow C'_2 \cdots C'_{L^3-1} \rightarrow C_1$. A set of L^3 moves constitutes a Monte Carlo sweep (MCS). In the first MCS, since g_i is the same for all i , every move gets accepted.

At the end of the MCS, let us say the system is in microstate C_1 . Let $E(C_1)$ belong to the k th energy bin. We update g_k to $f \times g_k$, where $f=f_0$. The updated $\{g_i\}$ becomes operative for deciding acceptance or rejection in the next L^3 moves that constitute the next MCS leading to C_2 . Thus we get a chain of microstates $C_0 \rightarrow C_1 \rightarrow \cdots C_N$. We take $N = 10\,000$. Generating a Markov chain of length N constitutes one iteration. For the next iteration we change f to $f^{0.9}$. The microstate generated at the end of an iteration forms the initial microstate for the next. Also the updating of the density of states is continued from one iteration to the next. We carry a total of M iterations and this constitutes a Wang-Landau (WL) run, see below. In the last iteration of a WL run, we have $f=f_M=f_0^{\mu(M)}$, where $\mu(M)=(0.9)^M$. We have chosen $M=160$ so that $f_M-1 \approx 10^{-7}$ for $f_0=10$.

We start a WL run with f reset to f_0 . The microstate generated at the end of a WL run is taken as the initial microstate for the next. Similarly the updated density of states $\{g_i\}$ at the end of a WL run provides the initial density of states for the next. We carry out a total of 50 WL runs. The value of f_0 is 100 for the first 40, 10 for the next 9, and $f_0=e$ for the last WL run.

The density of states at the end of 50 WL runs is taken as an input for a long non-Boltzmann sampling run of 2.5 million Monte Carlo sweeps, called the production run. Thus we get a g ensemble of microstates from which the desired macroscopic properties can be calculated by unweighting and reweighting.

We also found that it is imperative to employ numerical techniques that avoid overflow problems and the attendant loss of precision due to truncation. To this end, we adapted the techniques suggested by Berg [23]. These involve principally the following. Let $\alpha_i = \log g_i$ denote the microcanonical entropy. We define $\xi_i = \log \alpha_i$. We carry out all the calculations in terms of $\{\xi_i; i=1, 2, \dots, 9L^3\}$. We derive expressions for acceptance probability p in terms of $\{\xi_i\}$ and employ them in the simulation. Similarly we derive expressions for the updating of $\{\xi_i\}$ and for unweighting and reweighting, in terms of $\{\xi_i\}$. These are briefly described in the Appendix. Employing this modified Wang-Landau algorithm we simulated a lattice model of liquid crystalline system with $L=4, 6, 8, 10$, and 12 focusing on nematic-isotropic transition. We present the results in the next section.

IV. CHARACTERISTICS OF BULK LIQUID CRYSTALS

The orientational order parameter S of a microstate is defined as follows. Let $|u_i\rangle$ denote the spin at the i th lattice site. We first construct an average projection operator for a microstate C given by

$$A(C) = \frac{1}{L^3} \sum_{i=1}^{L^3} |u_i\rangle \langle u_i|. \quad (11)$$

From A we construct a traceless symmetric tensor,

$$Q(C) = A - \frac{1}{3} \text{trace}(A) \times I, \quad (12)$$

where I denotes a unit matrix. Let $\lambda_{\max}(C)$ denote the largest eigenvalue of Q . Then $S(C) = 3\lambda_{\max}(C)/2$. The corresponding eigenvector $|\lambda_{\max}\rangle$ defines the director for the microstate C .

Figure 1 depicts $\langle S \rangle$ as a function of temperature for system sizes $L=4, 6, 8, 10$, and 12. We observe that the modified Wang-Landau Monte Carlo simulation predicts correctly the transition from a high temperature disordered (isotropic) phase to a low temperature nematic phase. For $L=4$ the transition is not sharp, due to finite size effects. However when we increase the system size, the transition becomes sharper.

Next we investigate the behavior of specific heat at constant volume, C_V as a function of temperature. C_V is calculated from energy fluctuations and is given by

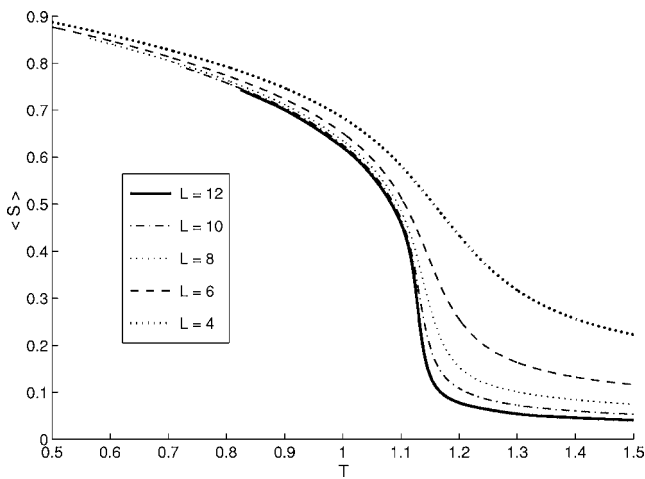


FIG. 1. The orientational order parameter S versus temperature (in units of dimensionless energy, with $k_B=1$) for $L=4, 6, 8, 10,$ and 12 . The transition becomes sharper with increase of system size.

$$C_V = \frac{\langle E^2 \rangle - \langle E \rangle^2}{k_B T^2}. \quad (13)$$

The results are depicted in Fig. 2. As L increases the C_V profile becomes sharper. Also the temperature $T_{NI}(L)$ at which the specific heat is maximum, shifts slightly to lower values, as expected. We find that $T_{NI}(L=12)$ calculated from the C_V is 1.126 and is in good agreement with the earlier estimates [24,25]. We can estimate the $L \rightarrow \infty$ limit of the transition temperature by finite size scaling discussed later.

The variation of average energy $\langle E \rangle$ with temperature is depicted in Fig. 3. This quantity decreases with decrease of temperature. At transition the fall is sharp for large L .

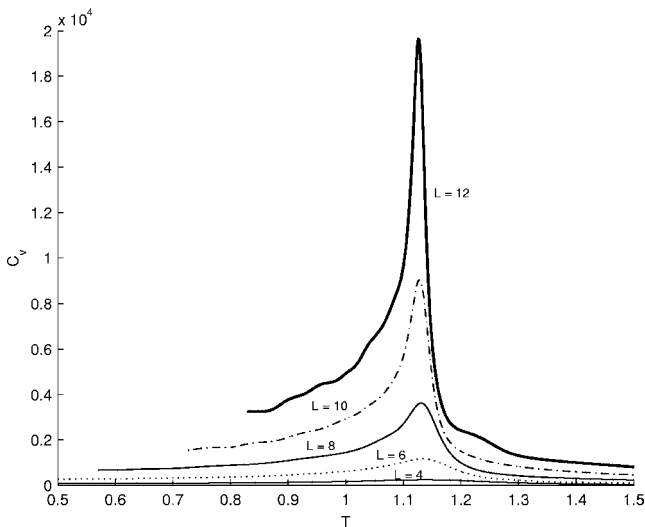


FIG. 2. Specific heat C_V [measured from fluctuations of dimensionless energy, see Eq. (13)] as a function of temperature (measured in units of dimensionless energy with $k_B=1$) for $L=4, 6, 8, 10,$ and 12 ; the transition becomes sharper with increase of system size; the transition temperature (the value of T at which the curve peaks) shifts to lower values with increase of system size.

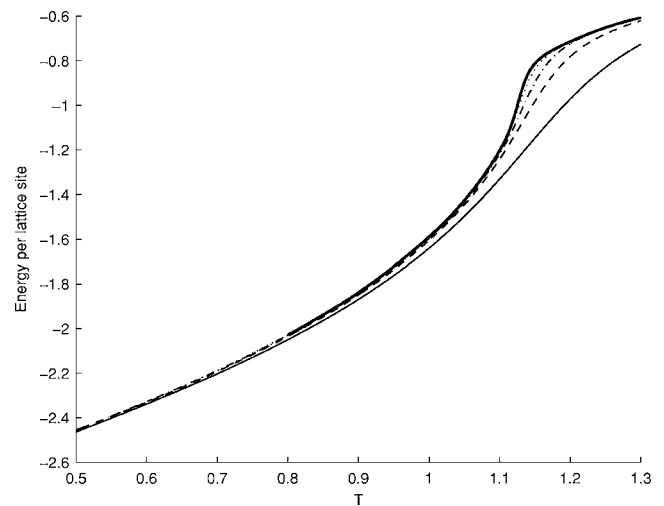


FIG. 3. Average (dimensionless) energy as a function of temperature (measured in units of dimensionless energy with $k_B=1$) for $L=4, 6, 8, 10,$ and 12 , from bottom to top, respectively. The transition becomes sharper with increase of system size.

We have calculated Binder's reduced fourth order cumulant of energy denoted by the symbol V_4 , see Ref. [15]. It is given by

$$V_4 = 1 - \frac{\langle E^4 \rangle}{3\langle E^2 \rangle^2}. \quad (14)$$

The variation of V_4 with T is depicted in Fig. 4 for $L=4, 6, 8, 10,$ and 12 . Each curve shows a minimum at an effective transition temperature. As the system size increases the effective transition temperature shifts to lower values as expected. Also $V_4 \rightarrow 2/3$ for $T \ll T_{NI}$ for all L considered and for $T \gg T_{NI}$ for large L . This is a clear signature of a first order transition.

Figure 5 depicts microcanonical entropy $\alpha = \log g$ versus E for system size $L=12$ on a log-linear graph. The results on entropy after successive WL runs are shown starting from the

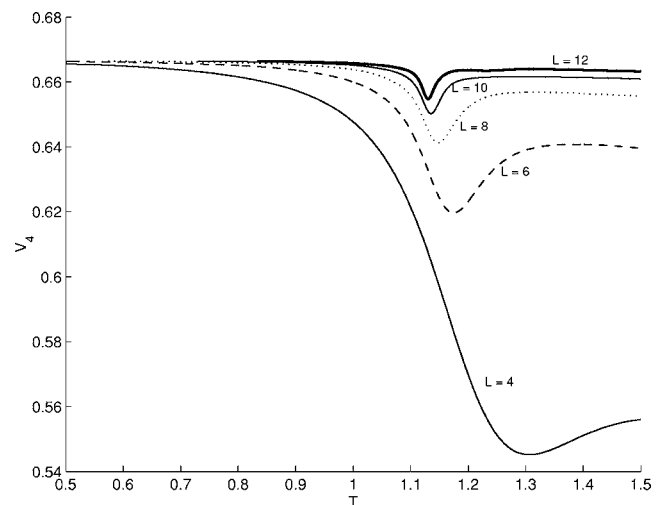


FIG. 4. Binder's fourth order cumulant of energy for $L=4, 6, 8, 10,$ and 12 . The behavior is indicative of first order transition.

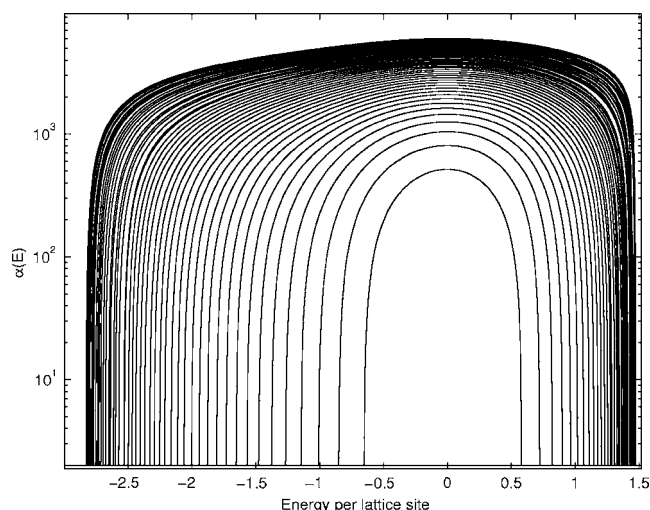


FIG. 5. Microcanonical entropy $\alpha_i = \log g_i$ as a function of dimensionless energy at the end of successive outer iterations starting from the inner most curve to the outer most. The data correspond to $L=12$ and are plotted on a log-linear curve. The shape of the curve will correspond to that of ξ employed in the simulation program. The logarithm of the outermost curve is taken as the input for a long production run which generates a g ensemble. Note that almost the entire energy range is spanned.

inner most curve and ending in the outer most. We see clearly that the range of energy spanned increases with increase of WL runs. The outer most curve is the output of the last WL run. The data on $\{\xi_i; i=1, 9L^3\}$ obtained at the end of the last WL run is employed in the long non-Boltzmann sampling run (production run) and a g ensemble of microstates is generated. All the quantities were calculated by unweighting and reweighting at temperatures spaced out with a fine resolution of 0.001.

Finally we have presented in Fig. 6 the finite size scaling of the transition temperature obtained from specific heat, orientational susceptibility, and the fourth order cumulant of Binder. The orientational susceptibility χ is calculated from the fluctuations of S and is given by

$$\chi = \frac{\langle S^2 \rangle - \langle S \rangle^2}{k_B T}. \quad (15)$$

The transition temperature is plotted against inverse of the volume of the system. The three curves scale linearly with $1/L^3$ and extrapolation ($L \rightarrow \infty$) gives an estimate of the nematic-isotropic transition temperature. $T_{NI}(L=\infty)$ estimated from specific heat data is 1.1284, from susceptibility data is 1.1299 and from the data on Binder's cumulant is 1.1211. These results are in good agreement with earlier estimates [24,25] up to second decimal.

V. CONCLUSIONS

We have demonstrated for the first time the applicability of the recently proposed Wang-Landau Monte Carlo algorithm to the study of liquid crystalline systems with continuous energy spectrum. We have made use of the flexibility of

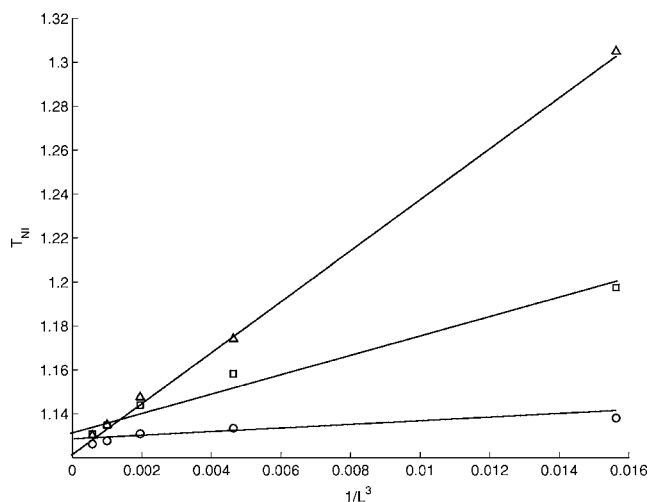


FIG. 6. The transition temperature (measured in units of dimensionless energy, with $k_B=1$), versus $1/L^3$. The top line with symbol \triangle corresponds to T_{NI} obtained from fourth cumulant of Binder; the middle line with symbol \square corresponds to T_{NI} obtained from the orientational susceptibility and the bottom line corresponds to the T_{NI} obtained from the specific heat. The value of T_{NI} in the limit $L \rightarrow \infty$ is given by 1.1284 from finite size scaling of specific heat data, 1.1299 from data on susceptibility and 1.1211 from data on Binder's fourth cumulant of energy.

the algorithm and studied nematic-isotropic transition in a three-dimensional lattice model of bulk liquid crystals. We have employed the Lebwohl-Lasher potential that has the head-tail flip symmetry of the nematic director and in which the energy varies continuously. For even moderately large system Wang-Landau dynamics becomes unacceptably slow. The density of states function $g(E)$ gets confined to a narrow energy range and becomes steep. As a result, the system spans only a restricted range of energy. Increasing the number of sweeps in an iteration does not seem to help. This slowing down of dynamics seems to be an inherent problem of this algorithm for such systems. Interestingly such problems do not arise for simulating systems with discrete energy spectrum, e.g., Ising and Potts spin models. To overcome these problems, we have proposed a few modifications to the Wang-Landau algorithm and demonstrated that these modifications help the basic algorithm to span larger regions of the energy space systematically. We have followed the strategy of calculating macroscopic properties from a production run carried out with the density of states obtained from the last of the Wang-Landau runs. The advantage of this strategy is that we need not insist on a strictly flat histogram of energy. An approximately flat energy histogram is adequate since the macroscopic properties are calculated by unweighting and reweighting of the microstates of the g ensemble. We have modified the Wang-Landau algorithm, details of which have been described in the paper. It is these modifications that have made possible simulation of the liquid crystalline system in which a spin is continuously orientable resulting in a continuous energy spectrum. We show that with the modifications of the Wang-Landau algorithm the macroscopic properties of bulk liquid crystalline system can be calculated with a good degree of accuracy and with vastly improved

temperature resolution. This opens up the possibility of exploiting the full power of the (non-Boltzmann) Wang-Landau Monte Carlo techniques to simulate several complex phenomena in liquid crystalline systems. Examples of such problems include phase transition in thin films deposited on substrates with complex geometry, study of polymer dispersed liquid crystals (PDLC) and effect of disorder and confinement on the nematic-isotropic phase transition. Work on these and related problems are in progress and will be reported soon.

ACKNOWLEDGMENT

The Monte Carlo simulations reported in this paper were carried out at the Centre for Modeling, Simulation and Design of the University of Hyderabad.

APPENDIX

Let g_i denote the number of microstates in the i th energy bin and $\alpha_i = \log(g_i)$ the corresponding microcanonical entropy. We define $\xi_i = \log(\alpha_i)$. In the program only the array

$\{\xi_i; i=1, 9L^3\}$ is stored, updated, and eventually employed in reweighting. All the required parameters like the acceptance probability p , and unweighting and reweighting factor W are calculated in terms of $\{\xi_i; i=1, 9L^3\}$.

First we initialize $\{\xi_i = \log(2) \forall i=1, 9L^3\}$. Let the energy of the current microstate belong to an energy bin c and the trial microstate, to an energy bin t . The acceptance probability of the trial state in the Wang-Landau algorithm is given by

$$p = \begin{cases} 1 & \text{if } \xi_t \leq \xi_c \\ \exp[-\exp(\xi_t + \log\{1 - \exp[-(\xi_t - \xi_c)]\})] & \text{if } \xi_c < \xi_t. \end{cases}$$

If the visited microstate has an energy falling in the say i th bin, then ξ_i is updated to $\xi_i + \log[\log(f)]$ where f is the Wang-Landau factor for that run.

The unweighting and reweighting of microstates belonging to the g ensemble are carried out as follows. Let C be the microstate under consideration. Let the energy $E = E(C)$ of the microstate fall in the bin c . Let ξ_c be the value of ξ in that bin. The weight factor $W(C)$ attached to $C \in g$ -ensemble is given by

$$W(C) = \begin{cases} \exp(+\exp[\xi_c + \log\{1 - \exp(-\Delta_1)\}]), & \text{where } \Delta_1 = \xi_c - \log(\beta E) \geq 0, \\ \exp(-\exp[\log(\beta E) + \log\{1 - \exp(-\Delta_2)\}]), & \text{where } \Delta_2 = \log(\beta E) - \xi_c \geq 0. \end{cases}$$

It is easily verified that the above weight factor is identical to the one given by Eq. (6) except that we have expressed it in terms of $\{\xi_i\}$ instead of $\{g_i\}$. The average of a macroscopic property O is calculated employing Eq. (7).

-
- [1] D. P. Landau and K. Binder, *A Guide to Monte Carlo Simulations in Statistical Physics* (Cambridge University Press, Cambridge, 2000).
- [2] K. P. N. Murthy, *Monte Carlo Methods in Statistical Physics* (Universities Press, India, 2004).
- [3] N. Metropolis, A. W. Rosenbluth, M. N. Rosenbluth, A. H. Teller, and E. Teller, *J. Chem. Phys.* **21**, 1087 (1953).
- [4] H. Müller Krumbhaar and K. Binder, *J. Stat. Phys.* **8**, 1 (1973).
- [5] R. J. Glauber, *J. Math. Phys.* **4**, 294 (1979).
- [6] M. Creutz, *Phys. Rev. Lett.* **43**, 553 (1979).
- [7] K. Kawasaki, in *Phase Transitions and Critical Phenomena*, edited by C. Domb and M. S. Green (Academic, London, 1972), Vol. 2.
- [8] R. H. Swendsen and J.-S. Wang, *Phys. Rev. Lett.* **58**, 86 (1987); U. Wolff, *ibid.* **62**, 361 (1989); R. G. Edwards and A. D. Sokal, *Phys. Rev. D* **38**, 2009 (1988).
- [9] L. D. Fosdick, *Methods Comput. Phys.* **1**, 245 (1963).
- [10] G. Torrie and J. P. Valleau, *Chem. Phys. Lett.* **28**, 578 (1974).
- [11] B. A. Berg and T. Neuhaus, *Phys. Lett. B* **267**, 249 (1991); *Phys. Rev. Lett.* **68**, 9 (1992).
- [12] J. Lee, *Phys. Rev. Lett.* **71**, 211 (1993); **71**, 2352 (1993).
- [13] F. Wang and D. P. Landau, *Phys. Rev. Lett.* **86**, 2050 (2001); *Phys. Rev. E* **64**, 056101 (2001).
- [14] P. A. Lebowitz and G. Lasher, *Phys. Rev. A* **6**, 426 (1972).
- [15] M. S. S. Challa, D. P. Landau, and K. Binder, *Phys. Rev. B* **34**, 1841 (1986).
- [16] D. Jayasri, V. S. S. Sastry, and K. P. N. Murthy, *Wang-Landau Monte Carlo simulation of isotropic-nematic transition under confinement*, 22nd International Conference on Statistical Physics, Bangalore, July 4-9, 2004.
- [17] M. S. Shell, P. G. Debenedetti, and A. Z. Panagiotopoulos, *Phys. Rev. E* **66**, 056703 (2002).
- [18] Q. L. Yan and J. J. de Pablo, *Phys. Rev. Lett.* **90**, 035701 (2003).
- [19] R. Faller and J. J. de Pablo, *J. Chem. Phys.* **119**, 4405 (2003).
- [20] G. Brown and T. C. Schutthess, *J. Appl. Phys.* **97**, 10E303 (2005).
- [21] N. Rathore, T. A. Knotts IV, and J. J. de Pablo, *Biophys. J.* **85**, 3963 (2003).
- [22] J. A. Barker and R. O. Watts, *Chem. Phys. Lett.* **3**, 144 (1969).
- [23] B. A. Berg, cond-mat/0206333 (unpublished).
- [24] U. Fabbri and C. Zannoni, *Mol. Phys.* **58**, 763 (1986).
- [25] N. V. Priezjev and R. A. Pelcovits, *Phys. Rev. E* **63**, 062702 (2001).